Magnetic and Mössbauer characterization of the discontinuous high-spin ($^6A_1$) ⇄ low-spin ($^2T_2$) transition in solid bis(pyridoxal 4-phenyl-thiosemicarbazonato)iron(III) chloride

Niranjan S. Gupta, Madan Mohan*
Department of Chemistry, N.R.E.C. College, Khurja (U.P.) 203131 (India)

Narendra K. Jha
Department of Chemistry, Indian Institute of Technology, Hauz Khas, New Delhi 110016 (India)

and **William E. Antholine**
National Biomedical ESR Center, Department of Radiology, Medical College of Wisconsin, Milwaukee, WI 53226 (U.S.A.)

(Received November 12, 1990)

Abstract

The iron(III) complexes [Fe(HPhthsa)$_2$]Cl, [Fe(HEtthsa)$_2$]Cl and [Fe(HMethsa)$_2$]Cl were synthesized and the phenomenon of discontinuous spin transition between the high-spin ($^6A_1$, $S=5/2$) and the low-spin ($^2T_2$, $S=1/2$) states in [Fe(HPhthsa)$_2$]Cl was confirmed by the measurement of temperature dependent magnetism and Mössbauer spectra. The tridendate ligands used were pyridoxal 4-phenyl-thiosemicarbazone (H_2Phthsa), pyridoxal 4-ethylthiosemicarbazone (H_2Etthsa), and pyridoxal 4-methylthiosemicarbazone (H_2Methsa). The magnetic moments for the spin-crossover complex show a thermal hysteresis of width $\Delta T \approx 9$ K with the transition centered at $T_c^{\uparrow} \approx 299$ K for increasing temperature and at $T_c^{\downarrow} \approx 290$ K for decreasing temperature. Variable temperature ^{57}Fe Mössbauer results also provide evidence for the presence of a first order phase transition in this complex. The first order (cooperative) nature of the spin-crossover transformation most likely occurs through the extended coupling of ferric complexes via intermolecular H bonds. The EPR results indicate that the ground state is a well separated Kramers doublet in the low-spin complexes.

Introduction

Transition metal complexes with d^4–d^8 electron configuration are capable of exhibiting a spin-crossover (so called spin-transition or spin-equilibrium) phenomenon, when the difference between the net ligand field strength and the mean pairing energy, after considering other relevant perturbations such as low field components, spin–orbit interactions, and covalency effects, become comparable to the thermal energy, K_BT [1–4]. The spin-crossover characteristics of the complexes in the solid state mainly show either a continuous (gradual) transition over a wide temperature range or a discontinuous (abrupt) transition within a few degrees at a certain critical temperature [1, 2].

*Author to whom correspondence should be addressed. Present address: Department of Chemistry, Southwest Texas State University, San Marcos, TX 78666, U.S.A.

The continuous spin-crossover behaviour has been studied for a significant number of iron(III) complexes [5]. For systems displaying continuous spin-crossover transitions, individual X-ray diffraction patterns are not obtained for the high-spin and the low-spin constituents. The observed line intensities in the pattern are independent of the temperature while the interplanner spacings, d_{hkl}, vary continuously with the temperature. The variations are consistent with volume changes associated with high-spin and low-spin isomers. These observations are in keeping with the formation of a random solid solution of the two spin isomers within the same lattice. It has been suggested that the continuous spin-crossover transitions involve weak cooperative interaction between the individual complexes and a wide distribution of the nuclei of the minority spin constituent.

The discontinuous spin-crossover transitions are encountered with iron(III) complexes which display a cooperative interaction between the individual complexes. Variable-temperature X-ray powder dif-

0020-1693/91/$3.50

fraction techniques have revealed that the transition is associated with a crystallographic phase change, which may be responsible for the abrupt change in spin transition [6–8]. The results have been interpreted in terms of a pronounced domain formation by both the minority and majority phases. Observations of thermal hysteresis [1], as well as a very few heat capacity investigations [9–11] identified most of these spin transformations as thermodynamically first order phase transitions [12].

Of the variety of six-coordinate ferric spin-crossover compounds investigated so far [5], the ferric thiosemicarbazones, particularly those formed with pyruvic acid thiosemicarbazone (**I**) and salicylaldehyde thiosemicarbazone (**II**), are unique in that they show a relative abundance of discontinuous spin-crossover transitions [13–20]. The spin-crossover transitions in these complexes are greatly influenced by the change in outer sphere cation Y, the number of water molecules, and the nature of substituent X attached to the salicylaldehyde moiety.

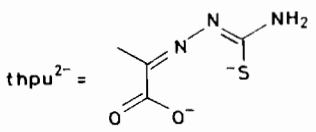

$Y[Fe(thpu)_2]\cdot \underline{n}H_2O$

I

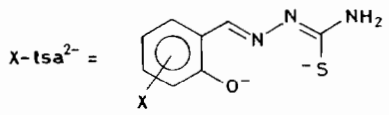

$Y[Fe(X\text{-}tsa)_2]\cdot \underline{n}H_2O$

II

Variable temperature single crystal X-ray structures have also been reported for several of the ferric salicylaldehyde thiosemicarbazone compounds [21–23]. Recently, Timken *et al.* [24] have reported the magnetic, spectroscopic and structural characterization of the discontinuous ferric spin-crossover complex [Fe(Hthpu)(thpu)], where $Hthpu^-$ and $thpu^{2-}$ are the deprotonated forms of pyruvic acid thiosemicarbazone. The compound shows a thermal hysteresis; the transition temperature is 225 K with sample cooling, and it is 235 K with sample heating.

The ferric complex $[Fe(HL)_2]Cl$ has been shown on the basis of variable temperature magnetic and ^{57}Fe Mössbauer measurements to exhibit an abrupt high-spin ($^6A_1$) ⇄ low-spin ($^2T_2$) transition (HL = deprotonated form of pyridoxal thiosemicarbazone (H_2L)) [25]. In the present contribution, a new discontinuous spin-crossover complex $[Fe(HPhthsa)_2]Cl$, where $HPhthsa^-$ is the anion of pyridoxal 4-phenylthiosemicarbazone, has been studied by variable temperature magnetic measurements and Mössbauer spectroscopy. In addition, the characterization of $[Fe(HEtthsa)_2]Cl$ and $[Fe(HMethsa)_2]Cl$ is also reported, where $HEtthsa^-$ and $HMethsa^-$ are the anion of pyridoxal 4-ethylthiosemicarbazone and pyridoxal 4-metylthiosemicarbazone, respectively.

Experimental

Compound preparation

Commercially available starting materials were used without further purification. Elemental analyses for C, H and N were carried out on a Perkin-Elmer model 240C automatic instrument.

Pyridoxal thiosemicarbazones

A solution of pyridoxal hydrochloride (0.21 g; 1 mmol), in its neutral form, in 30 ml of ethanol, was added with constant stirring to appropriate four-substituted thiosemicarbazide (1 mmol) in 30 ml of ethanol, and the solution mixture was heated under reflux for 30–40 min. After cooling a bright yellow microcrystalline product was isolated which was filtered off, washed with ethanol, and dried *in vacuo* over P_2O_5. Yield ≈90%. *Anal.* Calc. for $C_{15}H_{16}N_4SO_2$: C, 56.96; H, 5.06; N, 17.72. Found: C, 56.89; H, 5.04; N, 17.69%. Calc. for $C_{11}H_{16}N_4SO_2$: C, 49.25; H, 5.97; N, 20.89. Found: C, 49.19; H, 5.91; N, 20.84%. Calc. for $C_{10}H_{14}N_4SO_2$: C, 47.24; H, 5.51; N, 22.04. Found: C, 47.16, H, 5.49; N, 21.96%.

[Fe(HPhthsa)$_2$]Cl

A solution of anhydrous $FeCl_3$ (0.81 g; 5.0 mmol) in 20 ml of absolute ethanol was added to a hot suspension of pyridoxal 4-phenylthiosemicarbazone (0.32 g; 10.0 mmol) in 20 ml of absolute ethanol, and the resulting mixture was heated under reflux for 30 min. The thiosemicarbazone gradually dissolved and the dark brown crystals of the compound separated from the solution. The crystals were filtered off, washed with ethanol and diethyl ether, and dried *in vacuo* over P_2O_5. *Anal.* Calc. for $FeC_{30}H_{30}N_8S_2O_4Cl$: C, 49.89; H, 4.15; N, 15.52. Found: C, 49.82; H, 4.13; N, 15.45%.

[Fe(HEtthsa)$_2$]Cl and [Fe(HMethsa)$_2$]Cl

These complexes were prepared in the same manner as described above except that pyridoxal 4-ethylthiosemicarbazone (0.27 g; 10.0 mmol) or pyridoxal 4-methylthiosemicarbazone (0.26 g; 10.0 mmol) was used in place of pyridoxal 4-phenylthiosemicarbazone. *Anal.* Calc. for $FeC_{22}H_{30}N_8S_2O_4Cl$: C, 42.20; H, 4.79; N, 17.90. Found: C, 42.09; H, 4.69;

N, 17.82%. Calc. for $FeC_{20}H_{26}N_8S_2O_4Cl$: C, 40.16; H, 4.35; N, 18.74. Found: C, 40.12; H, 4.33; N, 18.69%.

Physical measurements

The magnetic susceptibility data on the polycrystalline materials at various temperatures (80–300 K) were obtained on a vibrating sample magnetometer, operated at 5 KG. The magnetic susceptibility data were calibrated with $CuSO_4 \cdot 5H_2O$, and a calibrated GaAs diode was used for sample temperature determination and control. For all data, diamagnetic corrections [26] were used in the calculation of molar paramagnetic susceptibilities.

Electron paramagnetic resonance data (X-band) were obtained on a Varian E-4 spectrometer, using DPPH as a reference material. Variable temperatures (300–77 K) were obtained with the use of a gas-flow cavity insert in conjunction with a Varian V-4540 temperature controller. Temperatures were determined before and after each spectra with a copper constantan thermocouple, and the temperature accuracy was estimated to be ±5 K. A direct immersion Dewar, which was inserted into the cavity, was used to obtain the spectral data at 77 K.

^{57}Fe Mössbauer spectral data were obtained on polycrystalline samples by using a constant-acceleration spectrometer that was calibrated with natural α-iron foil. The source was 50 mCi ^{57}Co in Cu and was maintained at room temperature for all experiments. Variable temperature measurements between 80 and 330 K were performed by using a custom made superinsulated cryostat, the temperature being monitored by means of a copper constantan thermocouple, mounted on the sample cell holder. The absolute precision is estimated to be ±3 K. A computer program was used to fit the Mössbauer absorptions to Lorentzian line shapes. All isomer shift values are reported with respect to the centroid of the spectrum of an iron foil enriched with ^{57}Fe at room temperature.

The solution conductivities were measured in MeOH containing (1×10^{-3} mol/l) at 25 °C by using a Toshiwal conductivity bridge, type Cl 01/01.

Results and discussion

The infrared spectra of solid pyridoxal 4-phenylthiosemicarbazone (H_2Phthsa), pyridoxal 4-ethylthiosemicarbazone (H_2Etthsa) and pyridoxal 4-methylthiosemicarbazone (H_2Methsa) exhibit absorption bands of ν(NH) and ν(NH^+) of the pyridine ring [27, 28] at *c.* 3140 m and 2800 mb, respectively, whose protonation has occurred due to the migration of the phenolic OH group to the pyridine nitrogen, but no ν(SH) at *c.* 2570 cm^{-1}. Thus, the free ligands exist in the thione form (**III**) in the solid state. However, in solution and in the presence of some metal ions the ligands may exist in equilibrium with the tautomeric form (**IIIa**). The tautomer (**IIIa**) by the loss of the thiol proton may act as a charged tridentate ligand coordinating to the metal ion through the mercapto sulfur, the azomethine nitrogen and the phenolic oxygen. When suspensions of the free ligands H_2Phthsa, H_2Etthsa and H_2Methsa in absolute ethanol were heated under reflux with an ethanolic solution of anydrous $FeCl_3$, dark brown microcrystals of $[Fe(HPhthsa)_2]Cl$, $[Fe(HEtthsa)_2]Cl$ and $[Fe(HMethsa)_2]Cl$ were isolated.

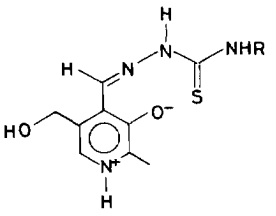

III

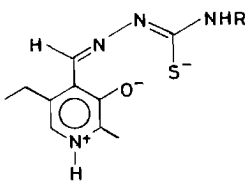

IIIa

R = Ph, Me or Et

All of these complexes are quite stable at room temperature and do not show any sign of decomposition after a long period of standing. All these complexes are insoluble in water, partially soluble in a large number of solvents of low coordinating ability like CCl_4, CS_2, C_6H_6, $C_6H_5NO_2$, $CHCl_3$, tetrahydrofuran, diethyl ether and acetonitrile, but highly soluble in a number of solvents of moderate-to-good coordinating ability like dimethylformamide, dimethylsulfoxide, methanol and pyridine. The molar conductance of the complexes in MeOH at *c.* 1×10^{-3} M lies in the 110–115 Ω^{-1} cm^2 mol^{-1} range indicating [29] their uni-univalent behaviour in solution. Although the complexes do not possess sharp melting points, they decompose near 240 °C.

Infrared spectra

The assignment of some of the main vibrational bands (cm^{-1}) of the free ligands and their ferric complexes are reported in Table 1. For all the ferric complexes the stretching vibrations of the NHR (R = $-C_6H_5$, $-C_2H_5$ or $-CH_3$) and OH (hydroxymethyl) groups appear in the range 3500–3200 cm^{-1}, while the spectral band of the NH group occurring at the frequency side (3140 cm^{-1}) in the free ligands disappears in the complexes, indicating the deprotonation of the NH group [30]. The coordination of the azomethine nitrogen atom to the ferric ion is confirmed by the displacement of the ν(N–N) stretching band towards the low frequency side from 1050 cm^{-1} in the free ligands to 1030 cm^{-1} and the shifting of the 1540 cm^{-1} band, assigned mainly to

TABLE 1. Selected vibrational bands (cm^{-1}) of H_2Phthsa, H_2Etthsa and H_2Methsa, and their iron(III) complexes

Compound	ν(NH) ν(OH)	ν(NH)	$\nu(NH^+)$	ν(C=N) ν(C=C)	Ring	ν(C=N)	Ring	(OH)	ν(C=O)	ν(N–N)	ν(C=S)
H_2Phthsa	3328s 3260m	3140m	2800mb	1620s	1580w	1540vs	1506w 1498s 1470m 1440m 1415m	1375vs	1290m	1050m	950m
[Fe(HPhthsa)$_2$]Cl	3460mb 3280m		2820w	1630s	1580s	1560s	1498s 1455m 1420m 1405sh	1375m	1310m	1030m	820m
H_2Etthsa	3330s 3260m	3140m	2800w	1610s	1575w	1535s	1500w 1498s 1470m 1440m 1410sh	1375s	1290m	1050m	930m
[Fe(HEtthsa)$_2$]Cl	3450mb 3270m		2800w	1620s	1570s	1560s	1498s 1450m 1418m 1405sh	1375s	1310m	1030m	825m
H_2Methsa	3328s 3260m	3140m	2800m	1618s	1580w	1540vs	1505m 1498s 1470m 1440m 1410m	1375s	1290m	1050m	932m
[Fe(HMethsa)$_2$]Cl	3440mb 3270m		2800w	1630s	1580w	1560vs	1498m 1470m 1420m 1405sh	1375s	1310m	1030m	820m

ν(C=N) stretching vibration in the free ligands, to the higher frequency side by approximately 30 cm^{-1} in the ferric complexes [31]. The shifting of the ν(C–O) phenolic stretching band from 1290 cm^{-1} in the free ligands to 1310 cm^{-1} in the complexes may be ascribed to a delocalization of electron density from the oxygen atom to the ferric ion, resulting from the slight ionic character of the C–O bond and consequently a slight shift in the ν(C–O) frequency [32]. The sharp band appearing at *c.* 930 cm^{-1} in the free ligands, and assigned to the ν(C=S) stretching vibration, shifts to a lower frequency side in the ferric complexes, indicating the coordination of the sulfur atom to the ferric ion. In the far-IR spectra, the ferric complexes exhibited bands at 425, *c.* 370 and *c.* 320 cm^{-1}, which are assigned to the νFe–S and νFe–N stretching vibrations, respectively.

Magnetic susceptibility

the variable temperature magnetic susceptibility data for $[Fe(HPhthsa)_2]Cl$ has been measured between 78 and 300 K for both increasing and decreasing temperature sequences. At 320 K, the effective magnetic moment $\mu_{eff}=5.90$ μ_B is a characteristic of a high-spin $^6A_1$ ground state, whereas at 78 K $\mu_{eff}=2.14$ μ_B implies a low-spin $^2T_2$ ground state. These values demonstrate that the spin transition is practically complete at both temperature extremes. The detailed magnetic data are given in Table 2, and the temperature dependence of μ_{eff} in the region of transition is illustrated in Fig. 1. It is evident from the data given in Table 2 and from Fig. 1 that the effective magnetic moment decreases smoothly from $\mu_{eff}=5.9$ μ_B at 320 K to 5.04 μ_B at 290.4 K, whereupon a sharp drop to μ_{eff} at 278 K is observed. Thus, on the basis of magnetism, the transition temperature associated with high-spin and low-spin transformation that occurs upon sample cooling may be estimated as $T_c^{\downarrow} \approx 290$ K. For the reverse transition, $T_c^{\uparrow} \approx 299$ K. A thermal hysteresis of 9 K is present. The abruptness of the transition and the observation of thermal hysteresis demonstrates that the transition is thermodynamically first order. The effective magnetic moment $\mu_{eff}=c.$ 2.12 μ_B over the temperature range 78–320 K studied for $[Fe(HMethsa)_2]Cl$ and $[Fe(HEtthsa)_2]Cl$ suggest that these compounds are predominantly in the low-spin state.

Mössbauer spectroscopy

The ^{57}Fe Mössbauer effect for $[Fe(HPhthsa)_2]Cl$ has been studied between 80 and 320 K for both increasing and decreasing temperature sequences. Figure 2 illustrates four representative spectra in the spin-transition region, i.e. those for 320.0, 292.5, 290.3, and 285.0 K, selected from a decreasing temperature series of measurements. It is apparent that

TABLE 2. Magnetic data for $[Fe(HPhthsa)_2]Cl$[a]

T (K)	$10^6 \times \chi_M$corr.[b] (cgs mol^{-1})	μ_{eff} (μ_B)	T (K)	$10^6 \times \chi_M$corr.[b] (cgs mol^{-1})	μ_{eff} (μ_B)
320.0	13487	5.90	265.2	2738	2.42
315.2	13461	5.85	280.0	2745	2.49
309.5	13569	5.82	285.1	2761	2.52
303.7	13591	5.77	287.5	2937	2.61
298.2	13746	5.75	289.0	3013	2.65
291.8	13999	5.74	292.2	3185	2.74
290.4	13580	5.64	295.5	3826	3.02
290.0	10817	5.03	296.0	4220	3.17
289.5	7808	4.27	296.5	4471	3.27
289.0	5778	3.67	297.5	6535	3.96
288.5	4024	3.06	298.8	10167	4.95
287.5	3285	2.76	300.0	13053	5.62
287.0	3010	2.64	302.7	13401	5.72
286.0	2930	2.60	303.2	13567	5.76
280.5	2807	2.52	307.5	13751	5.84
260.2	2860	2.45	313.6	13530	5.85
232.7	2867	2.32	318.7	13588	5.89
198.5	3247	2.28			
162.0	3909	2.26			
128.0	4561	2.17			
102.7	5580	2.15			
98.8	5801	2.15			
78.0	7279	2.14			

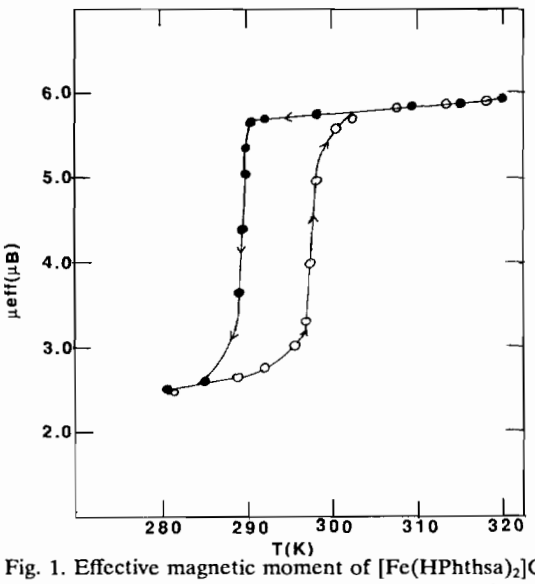

Fig. 1. Effective magnetic moment of $[Fe(HPhthsa)_2]Cl$ as a function of temperature. Both cooling (●) and heating (○) curves are shown. The solid lines are drawn for the purpose of clarity only and do not represent data fittings or simulations.

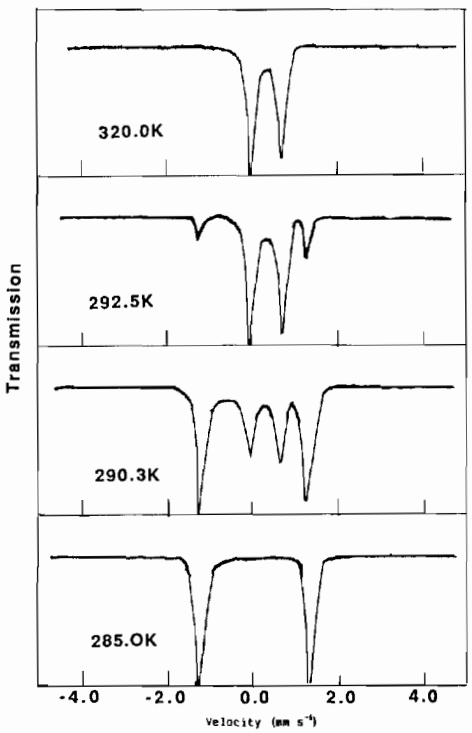

Fig. 2. Mössbauer-effect spectra of a powdered sample of $[Fe(HPhthsa)_2]Cl$ at 320.0, 292.5, 290.3 and 285.0 K.

for this sample the transition is complete at both extremes of this narrow temperature range. At 320.0 K, the lone doublet in the spectrum is characterized by the quadrupole splitting $\Delta E_Q = 0.85$ mm/s and isomer shift $\delta = 0.42$ mm/s and thus corresponds to

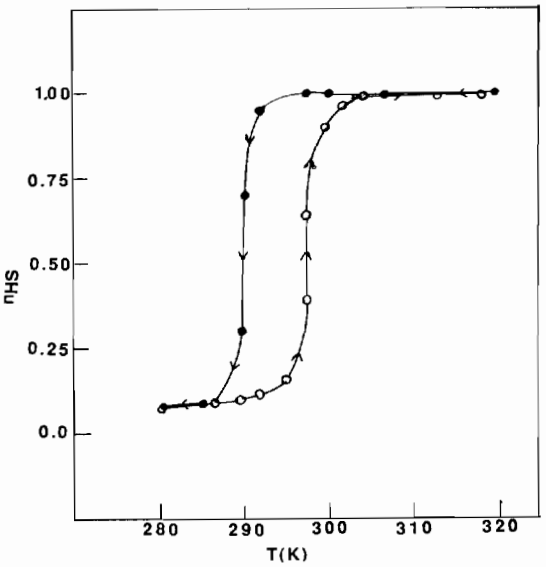

Fig. 3. Temperature dependence of the high-spin fraction (n_{HS}) for a powder sample of $[Fe(HPhthsa)_2]Cl$ on the basis of Mössbauer-effect measurements. A rising arrow indicates increasing temperatures, and a falling arrow indicates decreasing temperature ($T_c^{\uparrow} \approx 299$ K, $T_c^{\downarrow} \approx 290$ K). Data collected for increasing temperatures are marked with ○; those obtained with decreasing temperatures are marked with ●.

the high-spin ($^6A_1$) ground state of iron(III). As the temperature is lowered, another doublet with a much larger value of the quadrupole splitting and a smaller value of isomer shift appears; its intensity increases at the expense of the first doublet. At 290.3 K, the two doublets have almost equal areas, whereas at 289.1 K the relative contribution of the high-spin doublet has become very small. Finally, the lone doublet at 285.0 K is characterized by the quadrupole splitting $\Delta E_Q = 3.18$ mm/s and isomer shift $\delta = 0.19$ mm/s, and is assigned to the low-spin ($^2T_2$) ground state of the iron(III). These observations thus clearly indicate that in $[Fe(Hphthsa)_2]Cl$ the high-spin ⇄ low-spin transition is quite sharp and is complete within a temperature range of less than 5.0 K. The detailed value of the Mössbauer parameters are reported in Table 3. If the Mössbauer spectra are studied for increasing temperature, the transition is found to be centered at $T_c^{\uparrow} \approx 299.0$ K, whereas the transition temperature for decreasing temperature follows at lower temperature being centered at $T_c^{\downarrow} \approx 290.0$ K. The transition is therefore associated with a hysteresis of width $\Delta T_c \approx 9.0$ K; the hysteresis loop is illustrated in Fig. 3.

From Fig. 2, it is apparent that the two quadrupole doublets corresponding to the high-spin ($^6A_1$) and the low-spin ($^2T_2$) phase show a slight intensity asymmetry of opposite direction. This asymmetry

TABLE 3. Mössbauer effect parameters of $[Fe(HPhthsa)_2]Cl$ for a set of representative temperatures in the spin-transition region

T (K)	ΔE_Q ($^6A_1$) (mm/s)	IS ($^6A_1$) (mm/s)	ΔE_Q ($^2T_1$) (mm/s)	IS ($^2T_1$) (mm/s)	F(HS)	A^6A_1/A_{total}
Decreasing temperature						
320.0	0.85	0.42			1.00	1.00
310.7	0.85	0.41			1.00	1.00
300.3	0.84	0.41			0.98	1.00
292.5	0.84	0.42	3.12	0.21	0.94	0.98
290.3	0.84	0.43	3.11	0.20	0.68	0.56
289.1	0.83	0.44	3.12	0.21	0.50	0.12
288.2	0.81	0.44	3.16	0.19	0.31	0.06
285.0			3.18	0.19	0.07(5)	1.00
280.0			3.17	0.19	0.07(2)	1.00
Increasing temperature						
282.6			3.17	0.19	0.06(2)	1.00
285.0			3.16	0.19	0.08(0)	1.00
289.2	0.82	0.42	3.16	0.20	0.09(0)	0.01
292.3	0.83	0.40	3.14	0.20	0.11	0.02(5)
295.4	0.82	0.40	3.14	0.21	0.15	0.037(5)
297.3	0.83	0.41	3.13	0.20	0.38	0.37(5)
300.2	0.83	0.40			0.89	0.97(5)
302.4	0.84	0.40			0.95	0.98
303.7	0.84	0.41			0.98	0.99
307.5	0.83	0.41			0.99	0.99
312.5	0.84	0.40			0.99	1.00

could result from partial orientation of sample crystallites in the sample container, as observed for $Fe_2(CO)_9$ [33], or because of the Goldanski–Karyagin effect [34, 35]. This seems unlikely because the asymmetry tends to decrease with decreasing temperature, and the components are of equal area. It is therefore most likely that the observed asymmetry in the quadrupole split lines and its temperature dependence is consistent with intermolecular spin–spin relaxation [36].

The ^{57}Fe Mössbauer spectra of $[Fe(HEtthsa)_2]Cl$ and $[Fe(HMethsa)_2]Cl$ are measured at 300.0 and 78.0 K and the spectral parameters are detailed in Table 3. All the parameters are characteristic of low-spin ferric centers and indicate that the ground state is a singlet orbital (in the T_2 space) [37].

Electron paramagnetic resonance

The EPR spectra for $[Fe(HPhthsa)_2Cl]$, $[Fe(HEtthsa)_2Cl]$ and $[Fe(HMethsa)_2]Cl$ have been measured at 77 K in DMSO, and the spectra are illustrated in Fig. 4. The EPR signals of all these complexes are characterized by axial symmetry unless the low field component is too broad to detect. The g signal at 2.12 is interpreted in terms of a second minor species. The experimental anisotropic values for the low-spin state of these compounds are listed in Table 4, and are analyzed by following the method of Bohan [38] to determine the nature of the ground-state Kramers doublet. The high value of B_1 suggests that the ground-state Kramers doublet consists mainly of the state wherein the unpaired electron resides in the d_{xy} orbital. This is in agreement with the origin of the large quadrupole splitting for these compounds. Furthermore, the g-value analysis indicates that the first excited Kramers doublet of $^2T_{2g}$ is much higher in energy than the ground-state Kramers doublet (assuming spin–orbit coupling $Fe(III) \approx 460\ cm^{-1}$). This energy separation, much larger than the thermal energies, indicates that the low-spin magnetic moment and Mössbauer quadrupole splitting should be essentially temperature independent.

At ambient temperature we were unable to identify any signal as arising from the high-spin component. However, a strong signal at $g = 4.2$ was observed for $[Fe(HPhthsa)_2Cl]$ at low temperatures (Fig. 4). For simple high-spin low-symmetry ferric complexes the signals are typically located in the low-field region (1000–2500 G at X-band frequencies) because the zero field splitting in the high-spin state is gauged by $H = DS_z^2 + E(S_x^2 - S_y^2)$, where D and E are the axial and rhombic zero-field splitting parameters,

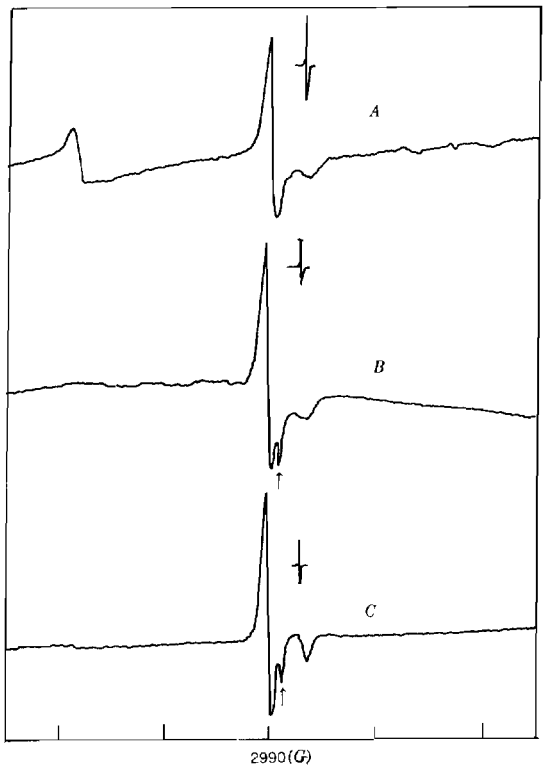

Fig. 4. X-band EPR spectra at 77 K for $[Fe(HPhthsa)_2]Cl$ (A), $[Fe(HEtthsa)_2]Cl$ (B) and $[Fe(HMethsa)_2]Cl$ (C). The presence of minor species is indicated by an arrow.

TABLE 4. Experimental and calculated ESR parameters

	$[Fe(HPhthsa)_2]Cl$	$[Fe(HEtthsa)_2]Cl$	$[Fe(HMethsa)_2]Cl$
g_x	2.16	2.16	2.16
g_y	2.16	2.16	2.16
g_z	1.99	1.96	1.97
A_1	0.111	0.130	0.124
B_1	1.00	0.994	0.996
C_1	0.00	0.000	0.000
δ/ζ	2.26	1.94	2.03
ϵ/ζ	0.00	0.000	0.000
E_1/ζ	−4.610	−3.967	−4.150
A_2	0.994	0.995	0.996
B_2	0.076	0.090	0.086
C_2	0.00	0.00	0.00
E_2/ζ	1.945	1.623	1.720
A_3	0.997	0.996	0.997
B_3	0.070	0.080	0.077
C_3	0.00	0.00	0.00
E_3/ζ	2.665	2.344	2.430

respectively [39]. A complex with low-symmetry (rhombic) exhibits an intense $g \approx 4.3$ signal if $E/D \approx 1/3$ and $h\nu/D \leqslant 3$, where $h\nu$ is the microwave energy (*c.* 0.3 cm^{-1} at X-band frequencies). At low temperature EPR signals at $g = c.$ 2.0 the ground-state Kramers doublet is well resolved and is characterized by axial symmetry in contrast to rhombic symmetry in a high-spin state. The difference of molecular symmetry between the low- and high-spin states play an important role in the spin-exchange mechanism. We attribute the absence of a high-spin signal at ambient temperature in $[Fe(HPhthsa)_2Cl]$ to short spin–spin relaxation times enhanced by short dipole–dipole (i.e. Fe–Fe) distances.

Conclusions

The discontinuous spin-crossover transitions are characterized by an abrupt change of relevant physical properties within a few Kelvin, thus a characteristic transition T_c exists or may be defined by that temperature where $^nHS = 0.50$. Spin-state transitions in compounds are accompanied by a significant modification of molecular dimensions, the most pronounced being the decrease in metal–ligand bond lengths on passing from high spin (hs) to low spin (ls), which generally results in a lowering of molecular volume.

Extensive hydrogen-bonding interactions have been noted [40, 41] in some metal complexes showing a spin-crossover behaviour which has led to the proposition that a change of hydrogen bonding may be important for the stabilization of one of the spin isomers. The ferric thiosemicarbazones are unique among spin-crossover complexes in that they possess an abundance of potential sites for intermolecule hydrogen bonding interactions [42, 43]. Thus, it is most likely that the cooperative (i.e. first order) nature of the spin-state transition in $[Fe(HPHthsa)_2Cl]$ is due to extended coupling of ferric complexes through intermolecular hydrogen bonds. This is certainly not applicable to the majority of the spin-state transitions since the intermolecular interactions undoubtedly depend upon subtle crystal packing and lattice properties, which are, to some extent, unique for each solid.

Acknowledgements

We are grateful for support from the Department of Science and Technology, New Delhi, India and NIH Grant RR 01008.

References

1 P. Gulitch, *Struct. Bonding (Berlin), 44* (1981) 83.
2 E. Konig, G. Ritter and S. K. Kulshreshtha, *Chem. Rev., 85* (1985) 219.
3 R. L. Martin and A. H. White, *Transition Met. Chem. (Weinhein Ger.), 4* (1981) 113.
4 E. Konig, *Prog. Inorg. Chem., 35* (1987) 527.
5 Y. Maeda and Y. Takashima, *Comments Inorg. Chem., 7* (1988) 41.
6 W. Irler, G. Ritter, E. Konig, H. A. Goodwin and S. M. Nelson, *Solid State Commun., 29* (1979) 39.
7 E. Konig, G. Ritter, W. Irler and H. A. Goodwin, *J. Am. Chem. Soc., 102* (1980) 4681.
8 E. Konig, G. Ritter, S. K. Kulshreshtha, J. Waigel and H. A. Goodwin, *Inorg. Chem., 23* (1984) 1896.
9 M. Sorai and S. Seki, *J. Phys. Soc. Jpn., 33* (1972) 575.
10 M. Sorai and S. Seki, *J. Phys. Chem. Solids, 35* (1974) 555.
11 V. I. Shipilov, V. V. Zelentsov, V. M. Zhadanov and V. A. Turdakin, *JETP Lett. (Engl. Transl.), 19* (1974) 294.
12 C. Kittel and H. Kroemer, *Thermal Physics,* Freeman, San Fransisco, CA, 1980, Ch. 10.
13 E. V. Ivanov, V. V. Zelentsov, N. V. Gerbeleu and A. V. Ablov, *Dokl. Chem. (Engl. Transl.), 191* (1970) 249.
14 E. V. Zelentsov, A. V. Ablov, K. I. Turta, R. A. Stukan, N. V. Gerbeleu, E. V. Ivanov, A. P. Bagdanov, N. A. Barba and V. G. Bodyu, *Russ. J. Inorg. Chem. (Engl. Transl.), 17* (1972) 1000.
15 V. V. Zelentsov, L. G. Bogolanov, A. V. Ablov, N. V. Gerbeleu and Ch. V. Dyatlova, *Dokl. Chem. (Engl. Transl.), 207* (1972) 864.
16 V. V. Zelentsov, G. M. Larin, E. V. Ivanov, N. V. Gerbeleu and A. V. Ablov, *Theor. Exp. Chem. (Engl. Transl.), 7* (1971) 648.
17 A. V. Ablov, V. V. Zelentsov, A. I. Shipilov, N. V. Gerbeleu and Ch. V. Dyatlova, *Dokl. Phys. Chem. (Engl. Transl.), 222* (1975) 567.
18 K. E. Turta, A. V. Ablov, N. V. Gerbeleu, Ch. V. Dyatlova and R. A. Stukan, *Russ. J. Inorg. (Engl. Transl.), 21* (1976) 266.
19 A. V. Ablov, V. I. Goldanskii, K. I. Turta, R. A. Stukan, V. V. Zelentsov, E. V. Ivanov and N. V. Gerbeleu, *Dokl. Phys. Chem. (Engl. Transl.), 196* (1971) 134.
20 N. A. Ryabova, V. I. Ponomarev, L. O. Atovmyan, V. V. Zelentsov and V. I. Shiplov, *Sov. J. Coord. Chem. (Engl. Transl.), 4* (1978) 95.
21 N. A. Ryabova, V. I. Ponomarev, L. O. Atovmyan and V. V. Zelentsov, *Sov. Phys.-crystallogr. (Engl. Transl.), 26* (1981) 53.
22 N. A. Ryabova, V. I. Ponomarev, V. V. Zelentsov and L. O. Atovmyan, *Sov. Phys.-crystallogr. (Engl. Transl.), 27* (1982) 46.
23 N. A. Ryabova, V. I. Ponomarev, V. V. Zelentsov and L. O. Atovmyan, *Sov. Phys.-crystallogr. (Engl. Transl.), 27* (1982) 171.
24 M. D. Timken, R. S. Wilson and D. N. Hendrickson, *Inorg. Chem., 24* (1985) 3450.
25 M. Mohan, P. H. Madhurnath, A. Kumar, M. Kumar and N. K. Jha, *Inorg. Chem., 28* (1989) 96.
26 B. N. Figgis and J. Lewis, in J. Lewis and R. G. Wilkinson (eds.), *Modern Coordination Chem.,* Interscience, New York, 1960, p. 403.
27 P. Domiano, A. Musatti, M. Nardelli, C. Pellizi and G. Prediere, *Transition Met. Chem., 4* (1979) 351.
28 Y. Matsushima, *Chem. Pharm. Bull., 16* (1969) 2143.
29 W. J. Geary, *Coord. Chem. Rev., 7* (1971) 81.
30 M. F. Iskander and L. El-Sayed, *J. Inorg. Nucl. Chem., 33* (1971) 4253.
31 M. Mohan, P. Sharma, M. Kumar and N. J. Jha, *Inorg. Chim. Acta, 125* (1986) 9.
32 M. Mohan, J. P. Tandan and N. S. Gupta, *Inorg. Chim. Acta, 111* (1986) 187.
33 T. C. Gibb, R. Greatrex and N. N. Greenwood, *J. Chem. Soc. A,* (1968) 890.
34 V. I. Goldanskii, G. M. Gorodinskii, S. V. Karyagin, L. A. Korytko, L. M. Kriahanskii, E. F. Makarov, I. P. Suzdalev and V. V. Khrapov, *Dokl. Akad. Nauk. SSSR, 147* (1962) 127.
35 S. V. Karyagin, *Dokl. Akad. Nauk. SSSR, 148* (1963) 1102.
36 M. Mohan, N. S. Gupta, A. Kumar and M. Kumar, *Inorg. Chim. Acta, 135* (1987) 167.
37 R. Zimmermann and H. S. Spiering, *Phys. Status Solidi (b), 67* (1975).
38 T. L. Bohan, *J. Magn. Reson., 26* (1977) 109.
39 H. H. Wickman, M. p. Klein and D. A. Shirley, *J. Chem. Phys., 42* (1965) 2115.
40 B. A. Katz and C. E. Strouse, *J. Am. Chem. Soc., 101* (1979) 6214.
41 M. Mikami, M. Konno and Y. Saito, *Chem. Phys. Lett., 63* (1979) 566.
42 M. Mathew and G. J. Palenik, *J. Am. Chem. Soc., 91* (1969) 6310.
43 M. Mathew and G. J. Palenik, *Inorg. Chim. Acta, 5* (1971) 349.